Functionalized graphene sensors for real time monitoring fermentation processes

Chinnathambi, Selvaraj

Chapter 2

Overview of miniaturised sensors for application in microbioreactors

2.1. Introduction

Development of fermentation processes in bioreactors usually requires many experiments because many conditions influence the outcome of a fermentation. If only a small number of reactors is available, the development takes a long time. If multiple reactors are available, laboratory space, investment and operating costs, and handling of the reactors by the researchers become more of a challenge. A possible solution could be downscaling of the reactors to make efficient use of space, labor, and investments. To ensure compatibility with commercially available analytical equipment and molecular/biochemical kits, the format of a microtiter plate (MTP) is preferred. Various commercially available MTPs exists with different heights and number of wells. The number of wells ranges from 6 to 3456, with volumes ranging from 17 ml to 2.7 µl.

Fermentation processes are highly sensitive to many process parameters that need to be measured online and controlled to specific set points. Among the process parameters, pH, dissolved oxygen (DO), biomass, and temperature are the main parameters that are of general importance. Hence the bioreactors should always be equipped with sensors to monitor the process parameters. In laboratory (bench-top) reactors with volumes from l to 10 liters, electrochemical sensors are used to monitor the pH and dissolved oxygen. For pH, glass-based electrodes are used, and Clark-type electrodes are used for DO measurements. These electrochemical sensors are difficult or impossible to use in small, MTP-based, microreactors because of size constraints.

Ion-Sensitive Field-Effect Transistor based electrodes (ISFET) have the potential to be used in microreactors because they can become very small. Commercially available ISFET pH sensors are successfully integrated with micro reactor arrays for process monitoring. The drift in voltage during the measurement was reported to be one of the problems associated with ISFET pH sensors. However, the drift is stable after two hours and is reproducible [1-5].

Optical sensors are another category of sensors that are available to detect pH and DO in microreactors. Optical pH and DO sensors have been successfully used and integrated with micro reactor arrays. The useful pH detection range is narrow for the optical pH sensor, and it is challenging to measure pH in processes carried out at pH <5 [6].

2.2. Fundamentals of sensing principles

Though there are many sensing methods available, only the sensing methods relevant for fermentation processes are considered here. As mentioned earlier, several parameters are important for fermentation processes. However, only the sensors available for crucial parameters like pH, DO, biomass, and temperature is mentioned in this chapter.

In this section, the fundamentals of an electrochemical sensors, optical sensors, impedimetric sensors, and chemiresistive sensors are discussed briefly.

2.2.1. Electrochemical sensors

There are two ways of how a signal is obtained from an electrochemical sensor, one is potentiometric, and another one is amperometric. In potentiometry, the potential of the working electrode is measured with respect to the concentration of an analyte when a fixed current is applied to the electrode. In amperometry, the current generated during the electrochemical reaction at the working electrode was measured at a fixed potential against the reference electrode. A typical electrochemical system is shown in Fig. 1. An electrochemical system

consists of three electrodes: the working electrode, the reference electrode, and the counter electrode. The potential applied to the working electrode is always referred to as a common reference electrode (Hg / $HgCl_2$, Ag/AgCl, reversible hydrogen electrode) [7-8].

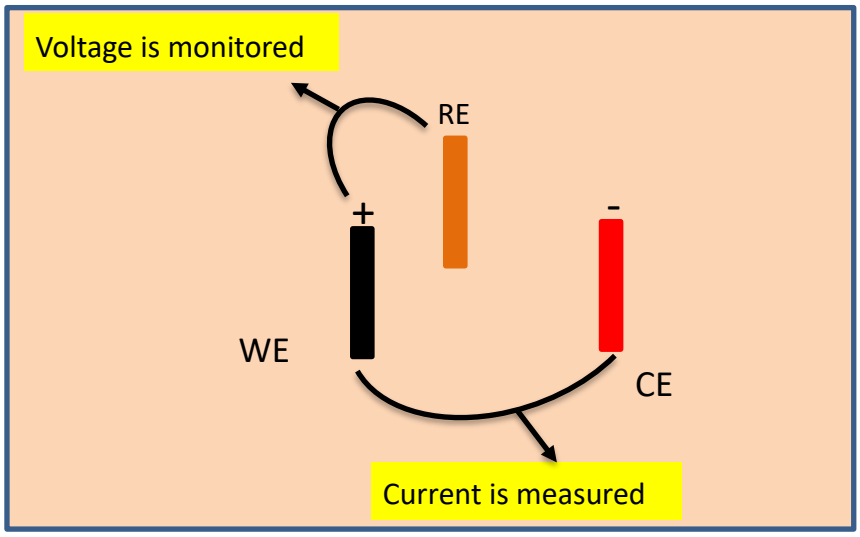

Figure 2.1: Schematic representation of an electrochemical cell. WE: working electrode; CE: counter electrode; RE: reference electrode.

2.2.1.1. The potentiometric method

In potentiometric methods, the equilibrium potential of the working electrode is measured. The potentiometric sensor is the basis of many electrochemical pH sensors. With this technique, the equilibrium potential of the ion selective electrode with respect to the Ag/AgCl reference electrode is measured. The equilibrium potential of a single electrode cannot be measured directly, and hence it is always connected with the non-polarizable electrode (reference electrode) that has a constant potential. The standard saturated calomel electrode (Hg / $HgCl_2$, SCE), and Ag / AgCl electrode are mostly used as reference electrodes. Traditionally, the indicator electrode, whose equilibrium potential needs to be measured, and the reference electrode are placed in different solutions that are separated by a salt bridge [7,8].

The equilibrium potential of the electrode varies with the activity of the ions that are present in the solution. The potential difference between the ion selective electrode and reference electrode occurs due to change in the activity of the ions according to the Nernst equation (Eqn.1).

$$E = E^o + \frac{RT}{nF}\, ln\frac{(a_o)}{(a_c)}$$ Equation 1

Where, E^o is the standard electrode potential, E is an equilibrium potential, a_o and a_c is the activity of oxidized and reduced species.

2.2.1.2. The amperometric method

In the amperometric method, the electrical current that arises from the electrochemical reaction of an electroactive species at the electrode surface is measured. The externally applied potential on the electrode with respect to the reference electrode drives the electrochemical reaction. The value of the current during the electrochemical reaction is directly proportional to the concentration of the electroactive species. The diffusion of the reactants from the bulk solution controls the concentration of the reactants at the electrode surface. The resulting current follows the Cottrell equation (Eqn 2.) [9,10].

$$I = \frac{nFACoD^{1/2}}{\pi^{1/2}t^{1/2}}$$ Equation 2

Where I is the current, n is the number of electrons, A is the area of the electrode, F is the Faraday constant, D is the diffusion coefficient, C_o is the concentration of the electroactive species in the bulk of the electrolyte, and t is time. Eqn. 2 is only applicable to planar electrodes. During amperometric detection, the electroactive species is reduced at the electrode surface, and a diffusion layer is formed due to the concentration gradient. The diffusion layer, and therefore the signal of the electrode, is flow dependent. An ultra-microelectrode can be used to mitigate the problem of the flow-dependent current response. In this case, the oxygen

concentration gradient is formed in a few milliseconds, and the diffusion of oxygen is so high that convection no longer affects the reduction process. For a circular-disc ultra-microelectrode, the Cottrell equation (Eqn. 3) becomes

$$I = nFAD\frac{C_o}{r} \qquad \text{Equation 3}$$

Where I is the current, n is the number of electrons, A is the area of the electrode, F is the Faraday constant, D is the diffusion coefficient, C_o is the concentration of the electroactive species in the bulk of the electrolyte, and r is the radius of the disc. Eqn. 3 indicates that the current response no longer depends on time [9-11]. For some microscale applications, an array of microelectrodes has been used to increase the sensitivity. When an array of electrodes is used, the electrodes should be positioned in such a way that the diffusion path of the electroactive species from the bulk solution to the individual electrodes is not merged [12-13]. Recessed electrodes are used to reduce the spacing between the electrodes. Recessing is also used in conventional Clark polarographic electrodes to avoid the usage of a polymer membrane. The recessed electrodes reduce the mass transport of electroactive species to the electrode surface, which depends on the height of the recess. The resulting current from recessed electrodes follows Eqn. 4 [14].

$$I = nFAD\frac{C_o}{r+h} \qquad \text{Equation 4}$$

Where I is the current, n is the number of electrons, A is the area of the electrode, F is the Faraday constant, D is the diffusion coefficient, C_o is the concentration of the electroactive species in the bulk of the electrolyte, r is the radius of the disc, and h is the height of the recess.

2.2.1.3 Ion-Sensitive Field-Effect Transistors (ISFET)

The construction of an ISFET is similar to a Metal-Oxide-Semiconductor Field-Effect Transistor (MOSFET). In a MOSFET a metal gate is deposited on top of an insulator (metal oxide) overlaying a semiconductor in which two metal connectors, a source, and a drain are

deposited. In the case of an ISFET, the potential of the gate is separated in the form of a reference electrode inserted in an aqueous solution which is in contact with the gate oxide. When an ISFET is exposed to an aqueous solution, the surface of the gate oxide is hydrated. The hydration of the gate oxide changes the concentration of the surface charge, which results in a different threshold voltage of the device. Hydration of the gate oxide is based upon the site-binding model [15-17]. To sense the ions of interest, an ion-selective membrane is placed over the gate to allow that only the specific ions are deposited on to the gate oxide [18-23]. A schematic representation of an ISFET pH sensor is shown in Fig.2.

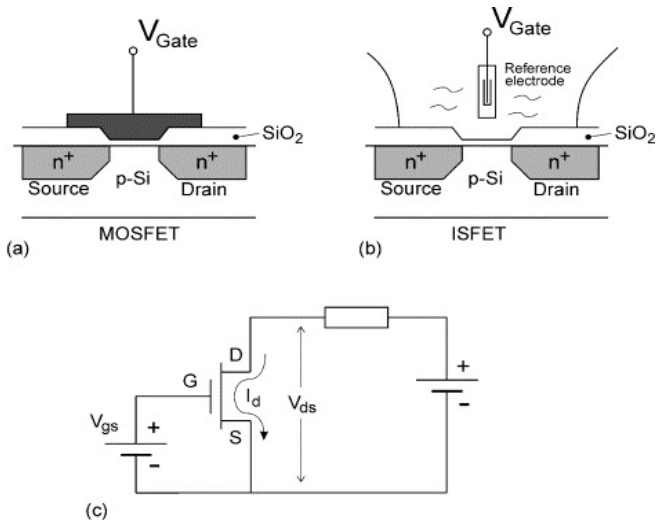

Figure 2.2: A **s**chematic representation of a MOSFET (a), ISFET (b), and an electrical circuit diagram of an ISFET pH sensor (c).

2.2.2. Optical sensors

Optical sensors are based upon a change in optical properties of indicator molecules dissolved in a solution or embedded in a polymer matrix. Absorption, fluorescent or luminescent properties of indicator molecules can be used to detect the presence of specific molecules and to determine their concentration. In the case of absorption, light is transmitted through a solution containing the indicator(s) and the transmitted light is detected with a light-dependent sensor (Light Dependence Resistor (LDR) or photodiode). The transmitted light has

the same wavelength but has a different intensity as the incident light from the source [24-26]. The molecule of interest may have the right spectral properties to be detected directly, e.g., pigments. Usually, a derivatization reaction with an indicator dye is necessary to use absorbance-based optical sensors.

Optical pH sensors do not measure the pH directly but measure the concentration of an indicator molecule whose optical properties are dependent on the pH [24-25]. In the case of fluorescence, an indicator molecule is excited at a particular wavelength and emits light at a wavelength higher than the wavelength of the excitation light [24, 27-28]. In pH measurements, the emission of the indicator molecule is related to the concentration of protons, hence with the pH. In DO measurements, quenching by oxygen of the emitted fluorescence intensity of an indicator molecule is used as the detection method. In general, optical sensors measure the activity of ionic sensing species (hydronium ion, pH) and for electron-neutral species like O_2 and CO_2 they measure the concentration [24].

Optical fiber sensors use two separate optical fibers to pass light to and from the sample, respectively. An LED is connected at the beginning of the fiber to send light to the sample. A photodiode is attached at the end of a second optical fiber to receive the light from the sample. Fiber optics are not disturbed by electronic noise, have no liquid junction problems, and there is no need for separate reference electrodes. However, optical sensors are sensitive to stray light, turbidity, and gas bubbles in the liquid [29].

In fluorescent sensing, different measurement methods are used. One is based on the luminescent intensity quenching due to radiation-less energy transfer and lifetime of the luminescence excite state (frequency-time domain) [30-32]. The ratiometric measurements are favored over single wavelength direct fluorescent sensing. The ratiometric method offers advantages like reduced interference, overcome photo bleaching, and photo stability issues of fluorescent dyes. The fluorescent dye molecule used for ratiometric sensing should have

overlapping excited and emitted wavelengths so that a single light source and photodetector can be used for the measurements. For fluorescence-based pH sensors, the frequency domain based dual lifetime referencing method is mostly used [33-35].

2.2.3. Chemiresistive Sensors

A chemiresistive sensor is based upon materials that show differences in the resistance/conductivity when the chemical environment changes. The resistance/conductivity change may occur due to swelling of the material, doping, and/or redox reactions with the analytes (Fig. 1.3). The conductivity of the material is measured by applying a constant voltage to the electrodes and measuring the resulting current. The conductivity of the material either increases or decreases depending upon the analyte interaction and results in a characteristic I-V curve. If the charge is removed from the material, the conductivity moves into the negative direction, and it moves toward the positive direction if electrons are injected into the material. The conductivity depends upon the surface charge of the molecules. The conductivity is related to the concentration of the surface charges.

2.3 Overview of miniaturised pH and dissolved oxygen sensors

2.3.1. Electrochemical pH sensor

The glass pH electrode is one of the most popular potentiometric pH sensor and consists of a pH-sensitive silicon membrane whose potential depends on the proton concentration. The glass pH electrode is the most preferred choice in industrial applications because of the high sensitivity and selectivity. However, the size of the rugged glass electrode and the requirement for frequent calibration does not allow it to use them in miniaturised applications, e.g., microreactors or other microfluidics devices. Instead, ion-selective membrane pH sensors and other electrochemical pH sensors have been used in miniaturised applications. In this section, an overview of electrochemical sensors and their use in microscale applications is given.

2.3.1.1. Polymeric membrane ion-selective electrodes

Conventional ion-selective electrodes (ISEs), e.g., glass electrodes, use a liquid contact for the ion to electron transduction. A solid Ag/AgCl electrode dipped in a chloride-containing electrolyte is used as the transducer for ion to electron transduction. Modern potentiometric ISEs use a solid-state electrode as the transducer that allows the fabrication of miniaturised ISEs. The solid-state transducer is coated between the ion-selective membrane and the conductive electrode. Several electro-active compounds are used as solid contact in ISEs, e.g., conductive polymers, carbon materials, and graphene.

The **i**on-selective membrane can be a thin film, as in the glass electrode, or an impregnated polymer matrix containing ionophores that react or form complexes with the analytes to give a potentiometric signal. Ionophores can be neutral, positively or negatively charged depending on the analyte of interest [36-40]. Polyvinyl chloride (PVC) is the most used polymer in ISEs, because of the high sensitivity and selectivity. However, poor biocompatibility, too brittle, less flexible are drawbacks of PVC. To make the PVC membrane more flexible, plasticizers are often used. Ion-selective polymeric membranes are a mixture of polymers, plasticizer, ionophores, and lipophilic salts. Lipophilic salts are used to delay the Donnan failure. The Donnan failure occurs due to the partition of opposite charges in the membrane after the attraction of analyte ions into the membrane. Several macrocycles and non-macrocycles based neutral carrier ionophores are developed for alkali and alkaline-earth metal ions based ISE's [41-48].

The first polymeric membrane pH-sensitive electrode that was developed used mesoxalonitrile p-(octadecyloxy)-m-chlorophenylhydrazone as the charged H^+ carrier. This charged ionophore was incorporated into a block copolymer matrix. Similarly, 3-hydroxy-N-dodecylpicolinamide charged H^+ carrier was used for a pH electrode with an extended pH range [49-51]. Simon et al developed a pH-sensitive electrode using tri-dodecylamine as a neutral charge carrier [52-57].

This neutral ionophore is incorporated into a PVC membrane and showed excellent sensitivity and selectivity within the pH range of 4.5 to 11.0. Many neutral ionophores (e.g., pyridines, piperazines, morpholines, imidazoles, pyrazoles, anilines, diamines) with different pKa values were tested to extend the working pH range of pH electrodes [57-60].

Ion-selective micro pH sensor

Ion-selective micro-electrodes to measure the pH in physiological applications are fabricated using double-barreled glass micropipettes. One of the barrels is used as the working electrode and is filled with pH-sensitive compounds. The other barrel is used as the reference electrode containing Ag/AgCl. Before filling, the working barrel was made hydrophobic by dipping into a trimethylchlorosilane solution. The working electrode is backfilled with a solution of ions to be measured, e.g., a NaCl solution to measure Na^+ ions. The reference barreled electrode is backfilled with a NaCl / KCl solution. The ion-selective micro pH sensor was used to detect pH changes in brain tissues [61]. The neutral carrier ionophores are mostly used to measure the pH in extra and intracellular applications.

Recently, a concentric ion-selective microelectrode was constructed to overcome the slow response time and high noise to signal ratio due to the electrical resistance of an ion exchange cocktail. Two thin borosilicate capillaries with different diameters were used to make a concentric ion-selective micro-electrode. The concentric ion-selective micro-electrode with fast response time and high sensitivity was used for *in vitro* extracellular studies. The microelectrode was fabricated, as shown in Fig. 4. The response time was obtained from constantly switching the pH solution from 7.42 to 6.87, and an average time constant of 14.9±1.3 ms with a sensitivity of 61.8±2.6 mV/pH was obtained. The applicability of this microsensor was studied in hippocampal slices of rat brain tissue [62].

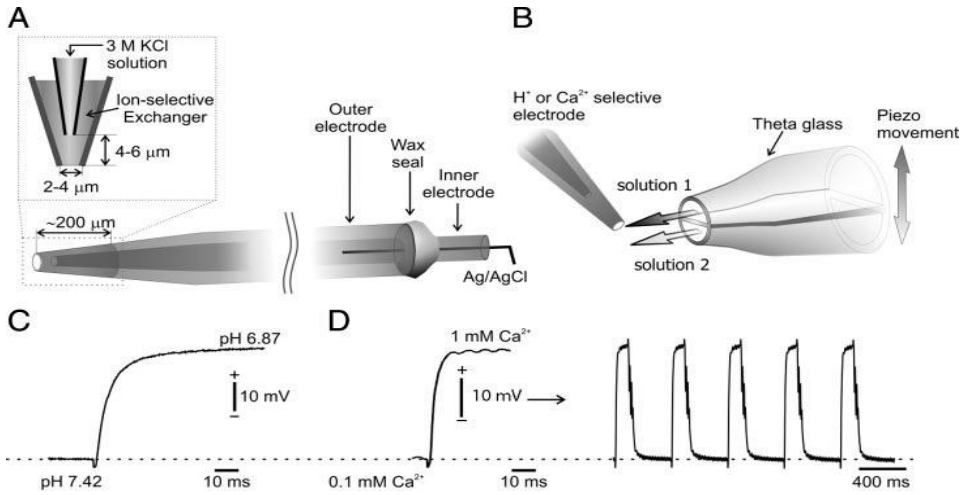

Figure 2.3: Double-barreled ion-selective polymer membrane micro-electrode for pH measurement (A), pH buffer solution dispenser for calibration set up (B), electrode response for H^+ (C) and Ca^{2+} (D) ions [62].

2.3.1.2. Solid-state metal oxide micro pH sensor

Solid-state metal oxide electrodes are another class of potentiometric sensors that can be miniaturised by microfabrication methods. IrO_2 is mostly used as the metal oxide electrode for pH sensing because of its wide pH range, a high sensitivity, and fast response time in combination with low potential drift. IrO_2 can be prepared in many ways, e.g., oxidation of an Ir microelectrode, anodic electrodeposition, thermal oxidation, or sputtering methods [63].

A solid-state IrO_2 micro-electrode array was fabricated on a silicon substrate and used to analyze tissue trauma during the implantation of a sensing probe. The micro-sized Ir array with an area of 700 μm^2 and with a 100 µm spacing was fabricated on a silicon substrate (Fig. 5). The iridium micro-electrode was electrochemically oxidized to form a multilayer hydrous iridium oxide layer. This IrO_2 micro-electrode showed a super Nernstian sensitivity of -90 mV/decade with reduced sensitivity of -85.8 mV/decade after exposing the electrode into a 0.1 M phosphate buffer solution. The micro-electrode showed good selectivity against Na^+, K^+,

Ca^{2+}, and Mg^{2+} ions, but it also showed a response in the presence of ascorbic acid. A Nafion dip-coating was applied to suppress the response towards ascorbic acid [64].

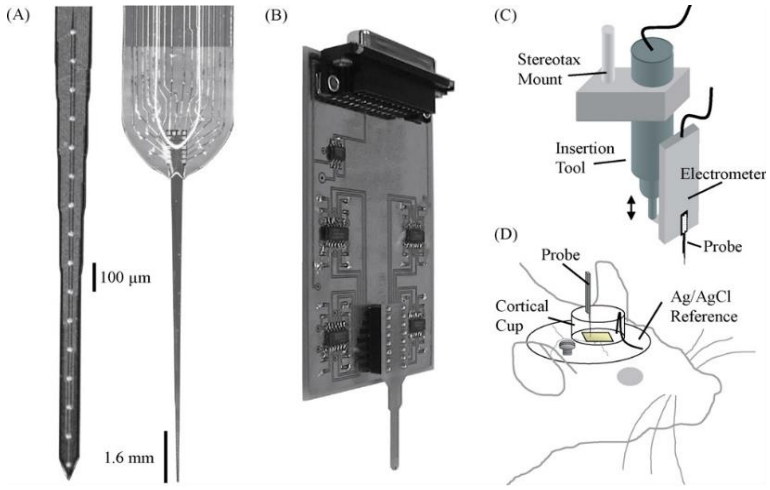

Figure 2.4: IrO_2 micro-electrode array on printed circuit board (A), micro-electrode connected to a circuit board for signal processing (B), automated insertion tool for insertion of the pH probe into tissues (C), and a cortical cup used for pH measurements (D) [64].

2.3.1.3. Ion-sensitive FET (ISFET) pH sensor

ISFET pH sensors are widely used as microscale electrochemical sensors in miniaturised applications. In an ISFET pH sensor, the gate oxide insulator is exposed to ions that are present in the test solution. The threshold voltage of the gate oxide changes when the gate oxide surface is hydrated. The adsorption of proton ions on the gate oxide layer is based on the site-binding model [65]. One of the disadvantages of ISFET pH sensors for long term application is that it shows transient behavior after a few hours of operation, this is called drift. However, the drift behavior is reproducible, and therefore, a correction can be used to overcome the drift problem [66]. There are several gate oxides insulators reported, e.g., SiO_2, Si_3N_4, Al_2O_3, and Ta_2O_5 [67-70].

ISFET pH sensor for miniaturised application

The micro ISFET pH sensor is used to monitor the pH in physiological applications and microfluidic devices. In general, the ISFET sensor has a miniaturised FET electrode, but it needs an Ag/AgCl reference electrode to control the gate potential. The attempt has been made to solve the problem of the reference electrode by placing it in a separate compartment bridged with the test solution. However, it is also possible to microfabricate the reference electrode along with the FET. Here an overview of recent research that used integrated ISFET pH sensor for physiological application is mentioned.

An ISFET pH sensor was used in real-time pH measurements of sweat in healthcare monitoring devices. An Al_2O_3 / SiO_2 di-electric layer was used as the pH sensitive membrane. The di-electric layer was deposited on top of an InGaZnO (30 nm) semiconductor channel that acted as the FET substrate (Fig. 6). The holes were created on the Al_2O_3 layer for the reference electrode. Subsequently, the Ag/AgCl reference electrode was printed and examined under an optical microscope. The sensitivity of the device for the pH was 51.2 mV / pH [65].

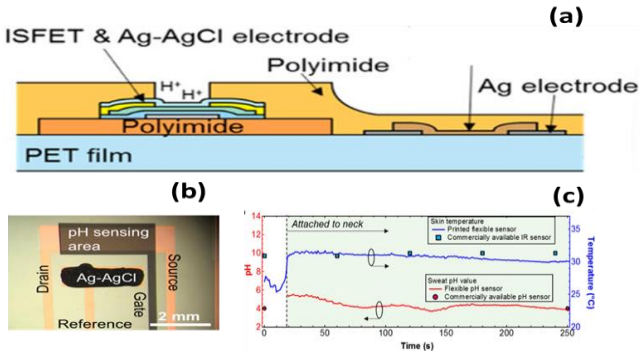

Figure 2.5: Illustration of ISFET device fabrication (a), Optical image of the reference electrode integrated in the ISFET device structure (b), and real time pH measurement from sweat (c).

An ISFET pH sensor was integrated within a micro fabricated cell culture platform [66]. The device was used to measure the rate of acidification in an extracellular medium. The pH was used to monitor biofilm formation and bacterial metabolic activities. A *Micrococcus luteus* biofilm formation was detected in a microfluidic environment using an ISFET pH sensor. The ISFET device was fabricated using a Ta_2O_5 membrane. The pH sensitivity of 50 mV/pH was obtained for pH range 4-8. The biofilm formation of *M. luteus* was detected by monitoring the acidification and alkalization of the culture medium during the growth. It was reported that biofilm formation occurs at the bottom of the microfluidic channel during the alkalization phase [67].

An ISFET pH sensor was also used to measure the bacterial activity of *Lactobacillus acidophilus* [68]. The activity of *L. acidophilus* was studied in different sugar solutions. *L. acidophilus* produces lactic acid during growth and decreases the pH of the medium. The PDMS based micro tank was created to reduce the volume of the sample to 1 µl. The micro ISFET pH sensor was fabricated on an n-type silicon substrate. SiO_2 and Si_3N_4 insulators were used as the pH-sensitive gate surface. Similarly, an ISFET pH sensor was used to monitor the metabolic activity of sugar fermentation during the growth of *Lactobacillus curvatus* and *Lactobacillus sakei*. An ISFET pH microsensor was used to differentiate between *L. curvatus* and *L. sakei* bacterium as both microorganisms have different metabolic activities for ribose fermentation.

2.3.1.4. Carbon fiber microelectrode voltammetric pH sensor

The carbon fiber (CF) micro-electrode is another miniaturized version of the sensor that is used in microscale physiological applications. Fast-scan cyclic voltammetry (FSCV) is often used for *in vivo* pH measurements. CF micro-electrodes are mainly used for real-time monitoring of the pH in brain tissue. CF is an attractive substrate because of its high conductivity, biocompatibility, high mechanical and chemical stability, and the surface can be easily functionalized. In addition to that, the small size of a CF microelectrode has an advantage that

it minimizes tissue damage, has a high spatial and temporal resolution and also can be used for longer time measurements [69].

CF microelectrodes are fabricated by the pulled capillary tube method (Fig. 7). Typically, 50-200 µm carbon fiber is extruded from a capillary tube and acts as the sensor probe. FSCV is used for detection of the pH. A cylindrical CF microelectrode with a length of 50-100 µm was prepared by sealing the CF in a capillary tube or pipette tip as shown in Fig. 7. The pH was detected by keeping the electrode at -0.6 V vs Ag / AgCl reference electrode, and then the electrode was fast scanned at 400 V/s back to 1.4 V in a triangular waveform. After subtracting the background current, differential pH values are obtained, absolute pH values can not be measured using this method [70].

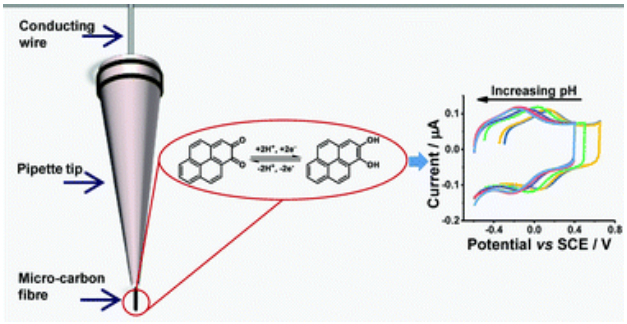

Figure 2.6: Illustration of voltammetric pH sensing using a carbon fiber microelectrode [71]

Modified cylindrical CF is investigated as a reagent-less sensing probe for real time measurement of pH in biological microenvironments. Fast blue RR salt (4-benzoylamino-2,5-dimethoxybenzenediazonium chloride hemi(zinc chloride) salt), a quinone-containing diazonium derivative, is electrochemically grafted on CF. The 5 µm wide and 200 µm long CF microelectrode was fabricated by aspirating 5 µm CF into a borosilicate capillary tube. FSCV was used for pH measurements. A sensitivity of 39 mV / pH was obtained for a pH range from 6-8.5 in adult hemolymph like (AHL) saline solution. This modified CF microelectrode was used to measure the *in vivo* pH change in descending neurons (DNs) from the fruit fly *Drosophila melanogaster* [71].

2.3.2. Electrochemical dissolved oxygen sensor

2.3.2.1. Amperometric dissolved oxygen sensor

There are several sensing methods available to detect dissolved oxygen (DO). Among them, electrochemical and optical sensors are preferred for online measurements. The Clark-type polarographic electrodes are amperometric sensors to detect DO. A Clark-type sensor consists of a cathode and an anode. Platinum is used as the cathode and Ag/AgCl is used as the anode. The platinum is separated from the solution by an oxygen permeable membrane. Dissolved oxygen diffuses through the membrane and is reduced at the platinum surface. During the reaction, the silver anode is oxidized and consumed. The electron flow (current) from the silver anode to the platinum cathode is used for the measurement. During the oxygen reduction reaction, oxygen is consumed at the electrode surface, and the concentration of oxygen reaches zero. In an unstirred solution, a concentration gradient is formed near the electrode, which is further extended to the bulk. It is a diffusion or Nernst layer. Hence, the current response of the electrode is controlled by diffusion. In a Clark electrode, a polymer membrane is used to separate the cathode from the solution, and the permeation of oxygen is directly proportional to the concentration of the oxygen in the solution. In an unstirred solution, the presence of the diffusion layer leads to erroneous DO values. This can be avoided by stirring the solution but the stirring rate affects the measurements as well. However, when using microelectrodes the effect of the stirring is minimal [10]. There are two ways DO microelectrodes can be fabricated, one is using pulled glass pipettes, and the second one is using lithographic microfabrication methods. In the next section, an overview of the development of microelectrodes and its physiological applications will be reported.

Microelectrodes for dissolved oxygen

Needle type recessed microelectrodes are mostly used to mitigate the problem of tissue damage, microcirculatory disturbance, and improved spatial resolution [75]. The recessed tip formation

overcomes the flow-dependent current response due to the reduced diffusion layer thickness. In a conventional DO microelectrode, the recessed cathode is prepared in a pulled glass micropipette with a tip of 2-5 µm. Then the pulled micropipette was half-filled with low-melting Bismuth alloy, and then gold was deposited on top of the alloy. The tip of the glass micropipette was recessed using 1 M KCN to dissolve part of the gold (Fig. 8b) [76].

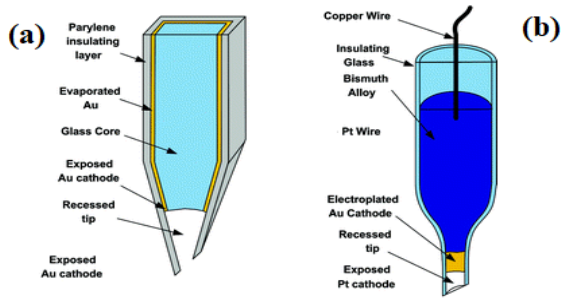

Figure 2.7: Recessed microelectrode fabrication using MEMS (a) and using conventional pulled capillary tip (b) [75]

The needle type DO micro electrode was fabricated using MEMS technologies [77]. The micro sized glass probes were diced from the wafer. The tip of the glass was etched by dipping in a mixture of HNO_3, H_2O_2, H_2O (10:7:33) to form a needle type micro electrode. The obtained 80 µm needle was further tapered down to 10 µm. Afterward, gold was deposited on either side of the glass probe and a Parylene insulating layer was formed on top of the gold layer. Finally, the recessed tip on the micro electrode was formed by HF etching (Fig. 8a). The needle type micro electrode showed a linear sensitivity of 147 pA/mg.L^{-1}. The conventional DO micro electrode was less sensitive with a slope of only 10 pA/mg.L^{-1}. The needle type micro electrode was used to study the DO-profile in a bacterial biofilm. The DO in the bulk solution was 8.5 mg.L^{-1}, which decreased to 5.9 mg.L^{-1} at the surface of the biofilm. At 700 µm inside the biofilm, no DO was detectable anymore [77].

In addition to Clark type polarographic electrodes, a three-electrode amperometric micro electrode was developed for dissolved oxygen measurements. These micro electrodes are fabricated using lithographic methods. Micro platinum or gold electrodes are patterned on a silicon substrate by photolithographic techniques.

Flow-dependent amperometric responses, which are observed in macro electrodes, are absent in micro electrodes. In the micro electrodes, the equilibrium oxygen concentration gradient is formed faster and the diffusion of the oxygen to the electrode is higher than the mass transport [10,78].

Krommenhoek et al. developed ultramicroelectrode arrays based on the amperometric DO sensor for online monitoring DO during yeast fermentation [10]. They formed 114 microelectrodes with a diameter of 2 µm. The spacing between the electrodes was 50 µm. The microelectrodes were formed by covering platinum with a 1 µm polyamide layer. This layer was used to create recessed electrodes to reduce the diffusion length. These ultramicroelectrodes have a 200 µm x 1000 µm platinum counter electrode. The microelectrodes responded linearly with the DO concentration, and a sensitivity of 3.7 $nA/mg.L^{-1}$ was obtained in the supernatant of a liquid yeast culture.

Similar, platinum ultramicroelectrode arrays were fabricated on a glass substrate and covered by silicone oxide – silicone nitrite – silicone oxide (ONO) insulating materials [78]. The insulating material was used to develop a recess on the electrode. The ultramicroelectrode disc was formed on 2 µm finger electrodes and the electrodes were separated 20 µm apart (10 times the electrode size). All the finger electrodes, containing equally spaced ultramicroelectrodes, were connected to a common platinum pad of 200 µm x 200 µm and the reference and counter electrode had the same size. The main importance of this study is that they used an ultra-short measurement time (< 3 ms) to measure the DO. The sensor response was reported as

$nAs^{-0.5}/mg.L^{-1}$. A sensitivity of 0.49 $nAs^{-0.5}/mg.L^{-1}$ was obtained in a phosphate buffer solution. The oxygen consumption during the measurement was 63 fmol or 10^{-6} % reduction of DO concentration in a 10 ml volume cell. Since this microelectrode array consumed less oxygen compared to a Clark micro electrode, it was proposed that the micro electrode could be used for DO measurements in biological samples in a confined environment such as in a microfluidic device. For example, in a 50 nL sample, minimal consumption of oxygen by the electrode is crucial as it could lead to low DO conditions of the sample.

The needle type integrated solid-state micro electrode is fabricated using photolithographic technology [79,80]. This integrated micro electrode contains a micro sized gold working and counter electrode and an Ag/AgCl reference micro electrode. Unlike other microsensors, where only the working electrode is miniaturised, the reference and counter electrode are also miniaturised and placed near the working electrode in this sensor. The electrodes are separated by 10 µm from each other. One of the advantages is that there is no need for a separate compartment for the reference and counter electrode. This needle type micro electrode was used to measure the oxygen distribution in aerobic granules consisting of consortia of microorganisms. However, these integrated micro electrodes are proposed to measure DO *in vivo/in situ* applications, the proximity of the counter and reference electrode created errors during the measurement.

Scanning electrochemical microscopy is another technique that utilizes a Pt micro disc electrode sealed in a glass pipette to monitor DO consumption in single living cells (mouse, bovine embryo). In this technique, the tip micro electrode is scanned in the XYZ direction to measure the oxygen reduction current that is related to the local distribution of dissolved oxygen [81-82].

2.3.3. Optical pH sensor

Optical pH sensors are called pH optodes and are based upon a change in the optical properties of indicator dyes. The indicator molecule is a weak organic acid that can reversibly bind protons. The optical properties of the indicator dye depend on the concentration of the protons present in the test solution. The pH optode takes advantage of different absorbance/fluorescence properties of an indicator (dye) molecule for its dissociated (base) and un-dissociated (acid) form. The degree of dissociation depends on the pH of the solution. The indicator molecules are embedded in a proton conducting polymer matrix. An optical sensor is used to measure the absorbance or fluorescence of the indicator dyes. The fundamental difference between a potentiometric pH electrode and a pH optode is that the electrode measures the activity of the hydronium ions while the optical sensor measure the concentration of protonated and deprotonated forms of indicator molecule [83]. In optical pH sensor, the linear relationship between indicator molecules and proton follows the Henderson-Hasselbach equation, as mentioned in eqn. 5

$$pH = pKa + \log [A^{-1}] / [HA] \qquad \textit{Equation 5}$$

Where $[A^{-1}]$, [HA] is a concentration of deprotonated and protonated form of indicator molecule, and pKa negative logarithm of dissociation constant.

The activity and concentration are linked by the activity coefficient (f) . Hence, taking activities into account, we get

$$pH = pKa + \log [A^{-1}] / [HA] + \log f_{A-1} / f_{HA} \qquad \textit{Equation 6}$$

The activity coefficient of the individual reactant approaches unity only in dilute solutions. Hence, an optical pH sensor is affected by ionic strength. As the activity coefficient is affected by ionic strength, the calibration curve is only valid for a given ionic strength and temperature of the calibration solution. Therefore, the correction needs to be performed before the

measurement of the test solution, whose ionic strength is unknown. The pKa of the indicator dye determines the characteristics of the optodes. The pKa determines the pH range in which the pH optode can be used. Only a pH range of pKa ± 1 can be measured with one indicator dye. For an extended pH range, more than one indicator dye needs to be used [84].

A fluorescent indicator dye is the most preferred molecule for an optical pH sensor because of its high sensitivity, selectivity, and no need to redirect incident light as it emits light in all directions. Because of the high sensitivity, minimal concentrations of fluorophores can be used in the polymeric matrix of the optode [85]. Frequently used fluorescent indicators are 1-hydroxypyrene-3,6,8-trisulfonic acid (HPTS), fluorescein, benzoxanthane, cyanine, seminaphtharhodafluors (SNARFs), and hydroxycoumarins based indicators dyes. These dyes are mostly excited in the visible region and emit around 500 nm. Fluorescein based indicators have the problem of photobleaching, and HPTS have high photostability but has an ionic strength dependent pKa. Coumarins based dyes consume more energy because they have excitation wavelengths between 350-450 nm.

One of the advantages of cyanine-based dyes is that they have an absorption/emission profile in the near-IR spectral regions. Near-IR chromophores are advantageous to use in biological samples as many biomolecules and cells have no absorption or fluorescence in that range, causing less interference. Boron−dipyrromethene or BODIPY dyes also have absorption/emission spectra in the near-IR region. A mixture of BODIPY with different pKa values was synthesized, and extended pH working ranges of 7-11 and 0-14 were reported [86].

Micro-optical sensor for miniaturized systems

Optical sensors can be prepared in several configurations, depending on the applications (Fig. 9). A sensor film of a few microns is prepared by drop-casting the polymer solution, containing the probe molecule, on to a micron to submicron-sized optical fiber tip. Instead of drop-casting,

dip-coating of the fiber tip into the polymer solution is also used. For some applications, micro/nanoparticles of the probe molecule are dissolved in the analyte [87].

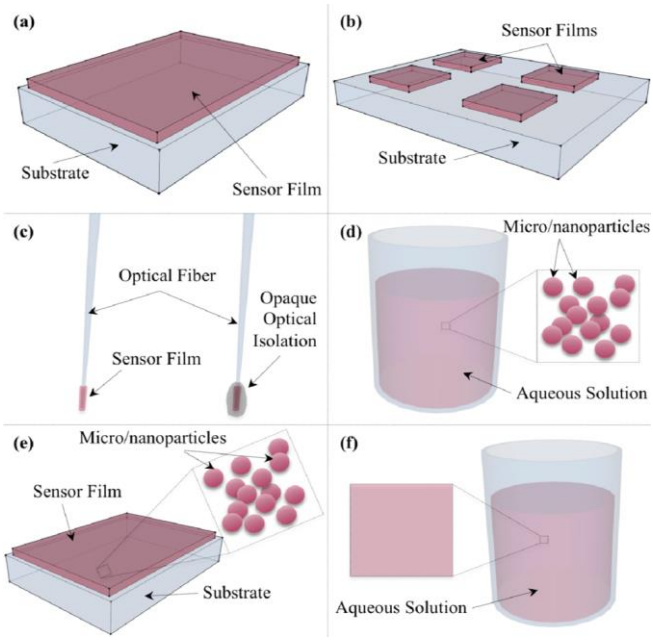

Figure 2.8: Different configurations of optical sensing probes. Thin film sensor (a), patterned thin-film sensor (b), dip-coated optical fiber sensor with and without optical isolation (c), micro and nano particles based optical probe suspended in aqueous solution (d), micro and nano particles probe suspended in a thin film (e), water soluble sensor probe dissolved in aqueous solution (f). [87]

Fiber optic micro pH sensor

In general, optodes for optical pH sensor are prepared by incorporating a pH-dependent fluorescence molecule in a proton-permeable membrane and fixed on the wall of the container that will be used for the pH measurement. For applications where sample volume is limited, the optical sensing probe needs to be miniaturised. The submicrometer range optical sensors that are needed to excite and read out the emission of the fluorescence molecule are developed by photo nanofabrication technology based on Near Field Optics (NFO) [88]. In this method, the

sensor matrix is synthesised using photopolymerization (Fig. 10). The NFO fiber tip is silanized and subsequently modified by the photosensitizer molecule (benzophenone). The sensitized NFO fiber tip is immersed in a monomer solution containing the pH-sensitive molecule, and the light is passed through the NFO and the light through the fiber initiates polymerization of the monomer solution. The result is that the pH-sensitive dye is covalently attached to the NFO tip embedded in a polymer matrix. The size of the polymer and the degree of polymerization is controlled by the time that the light is available. As the polymerisation of the sensor probe occurred in the presence of light, the sensing molecule is only attached to the surface of the fiber tip where the light emerges. In this way, a small, optical pH sensor can be easily prepared for pH measurements in low volumes.

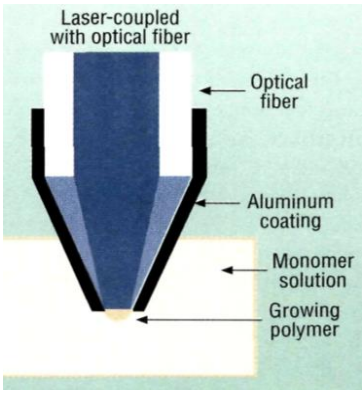

Figure 2.9: Image of an optical fiber tip during photo-polymerization of a sensor matrix [89]

Micro optical pH sensors can also be prepared by the dipping method, but the size of the sensor probe is less controllable, and it is more difficult to obtain well-defined sensing structures. In this method, the micrometer-size optical fiber tip is prepared by etching the end with concentrated hydrofluoric acid, or by laser-based puller, or by the fusion splicer technology [89-91].

The performance of an optical pH sensor is dependent on the sensor optode radius [89]. The absolute detection limit of a particular optical sensor decreases with r^3, and response time decreases with r^2. The signal to noise ratio drops with r^2. The lifetime of the sensor depends on the photobleaching of the pH-sensitive fluorescence molecule. Photobleaching has a considerable impact in smaller sized optical probes as the number of sensitive molecules is lower. There have been several strategies developed to mitigate the effect of photobleaching. For example, oxygen elimination, shorten excitation period, use of radiometric molecule or reference molecule, and usage of lifetime measurement instead of quenching [89].

Recently, a fiber-optic micro pH sensor based on a dual-emission sensitive dye was reported for applications in physiological conditions [91]. The dual-emission dye was reported to address pseudo pH changes that occur due to dye leaching or washout of the dye from the optodes that cannot be accounted in case of single emission sensitive dye optodes.

2.3.4. Optical DO sensor

Optical DO sensing is based on the luminescence quenching of metal complexes by an excited single (fluorescence) and/or triplet (phosphorescence) state of the oxygen molecule [89]. These oxygen-sensitive metal complexes are called lumophores. Lumophores are immobilized in an oxygen permeable polymer matrix. The dissolved oxygen diffuses through the polymer and interacts with the lumophores. The quenching of luminescence is linearly dependent on the concentration of oxygen present in the analyte. The quenching of lumophore intensity follows the Stern-Volmer equation (Eqn. 7 & 8) [89].

$$L^* + O_2 \xrightarrow[k_Q(O_2)]{} L + O_2^* \qquad \textit{Equation 7}$$

$$I_o/I = \tau_o/\tau = 1 + (K_{SV} \times pO_2) \qquad \textit{Equation 8}$$

Where I_o and I, and τ_o and τ, are the luminescence intensities and excited state lifetimes of the lumophore in the absence and presence of oxygen (L* and L in the reaction scheme, respectively), pO_2 is the partial pressure of the oxygen in the solution, K_{SV} the Stern-Volmer constant.

For optical DO sensing, several types of luminescent probes for DO sensing are available [92]. They can be classified into polyaromatic hydrocarbons (organic compounds, e.g., pyrene 1-butyric acid (PBA)), organometallic complexes (e.g., metal polypyridyl and metallo porphyrins). Mainly, Ru(II), Ir(II), Pt(II), and Pd(II) metal complexes are studied as fluorophores for optical DO sensing.

For an optical DO sensor, the luminescent probe molecules are embedded in an oxygen permeable polymer matrix to avoid direct contact of the fluorophores with the analyte medium. The polymer membrane also reduces the photobleaching effect. Several types of polymer membranes are used for the immobilization of the probe molecule [92]. Mostly, silicone polymers, organic polymers (polystyrene, poly (methyl methacrylate), and polyvinyl chloride), fluorinated organic co-polymer (polystyrene-2,2,2-trifluoro triethyl methacrylate and poly isobutyl methacrylate-co-2,2,2-trifluoro triethyl methacrylate), and cellulose derivatives (cellulose acetate and ethyl cellulose with embedded plasticizers (tributyl phosphate) are used [92]. Fluorinated polymers are preferred as the polymer matrix for optical oxygen sensing, because of its high oxygen permeability. Luminescent oxygen quenching of platinum and palladium octaethyl porphyrins (PtOEP and PdOEP) immobilized in poly(isobutyl methacrylate-co-trifluoro ethyl methacrylate) was reported [92-93]. Xiong et al prepared ruthenium (II) (2,2-bipyridyl) immobilized in a fluorinated xerogel film. They showed a good linear relation between the quenching of the lumophore and the oxygen concentration in the solution. A low detection limit of 0.04 ppm O_2 was achieved [94].

Fiber optic micro DO sensor

The fiber optic sensor, based on luminescence quenching of metal complexes, were used to detect DO in aqueous and biological samples [95]. Typical for the optical sensor is that the sensor spot of sensing material is fixed at the bottom or on the wall of the container and the measurement is carried out from the outside through a glass window. To measure DO in micro-reactors, a large sensor spot is not very useful. Also, detection of DO in tissue samples is not possible using sensor spots. A microsensor with a size of 25-200 µm is more suitable for this application [96-98].

Analogous to the optical pH microsensor, fiber optical microsensor for DO can also be prepared. The fiber end is modified with a probe molecule that is covalently linked within polymer matrix. The sensor was successfully used to measure the DO concentration in biological and living cells. Multimode and single mode optical fibers are used to fabricate the optical fiber microsensors. To achieve this, the end part of a micro-sized optical fiber (20-200 µm) is cleaved with an optical cleaver. Then, to construct the sensor, the cleaved optical fiber is pushed inside the polymer film embedded with the sensing molecule.

The submicron sized fiber optical microsensor is also prepared by tip modification at the end of optical fibers (Fig. 11). The tip is formed by drawing an optical fiber using an optical puller while heated with a CO_2 laser. The tapered pulled optical fiber forms a submicron sized tip. The optical fiber is silanized before dipping into a polymer solution containing the sensing molecules [97-99].

Ratiometric sensing becomes more prominent in optical sensors as it overcomes many problems that occur with single emission optodes [95, 99-102]. Kopelman *et al.* (2005) developed a ratiometric fiber optic microsensor for inter and intracellular dissolved oxygen measurements. The optical microsensor was prepared from multimode pulled and un-pulled optical fibers. The end part of the optical fiber was modified by repeatedly dipping the fiber in

an in optode film cocktail. The platinum (II) octaethylporphine (PtOEP) and Platinum (II) octaethylporphine ketone (PtOEPK) was used as the luminescence sensing material and platinum (II) octaethylporphine (OEP), Bodipy 577/618 maleimide was used as the reference dye. There was no difference observed in the sensing characteristics of the pulled and un-pulled fibers. Though, a two-fold increase in sensitivity of the pulled optical fiber tip was observed. This increased sensitivity was due to the reduced thickness of the sensor film that leads to a shorter oxygen diffusion length. A linear Stern-Volmer plot, as a measure of sensitivity, was obtained for dissolved oxygen concentration that ranges from 0 to 100 % O_2 saturation. The pulled fiber optical sensor showed a limit of detection of 14 ppb. For the un-pulled micro-optical sensor, this was almost 20 times higher, 260 ppb [95].

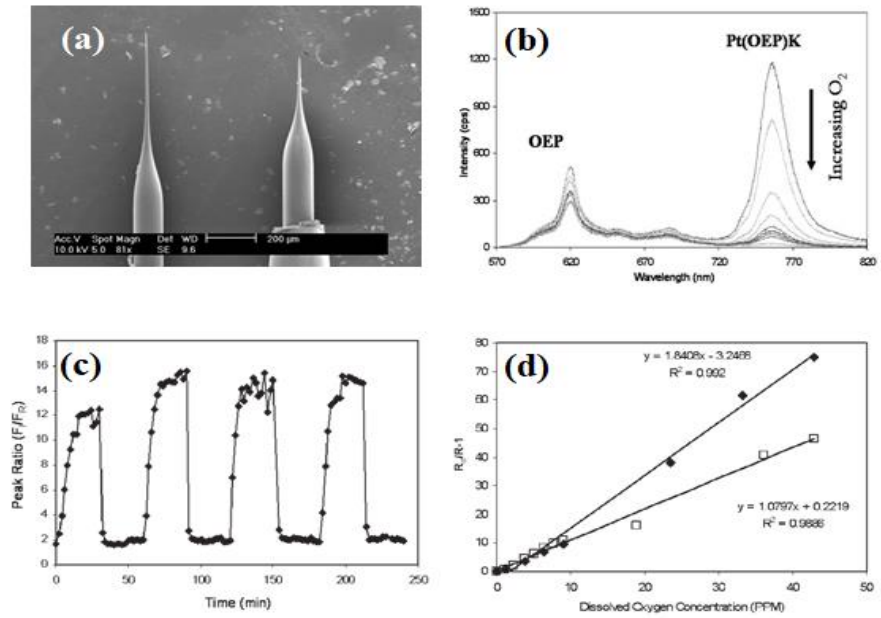

Figure 2.10: A: SEM image of sub-micron optical fiber tip (a), Luminescence spectra at different oxygen concentration (b), the reversibility of oxygen fiber sensor (c), and the Stern-Volmer sensitivity curve (d). [95]

This micro sensor was also tested to measure DO in the pancreatic islets of Langerhans, but inconsistent results were observed, and additional optimization of the fiber optical sensor was suggested.

Micro size sensor films containing a sensor probe immobilized in a polymer matrix were also developed to monitor DO in physiological applications. The Pt(II)-pentafluorophenylporphyrin fluorescent probe incorporated in a polystyrene polymer matrix was used to measure the respiratory activity of isolated mitochondria [103]. An optical sensor film that incorporated 8-hydroxy- pyrene-1,3, 6-trisulfonate (HPTS) and ruthenium-tris-4,7-diphenyl-1,10-phenanthroline- di-(trimethylsilylpropanesulfonate) was used to monitor the pH and DO simultaneously during the bacterial growth [104].

2.3.5. Biomass sensor

Biomass measurements are carried out by optical and electrochemical impedance spectroscopy techniques [105-108]. Optical measurements are based upon turbidity

measurement of the culture medium. The light is passed through the culture, and transmitted light is detected from the other end. When cell density increases, the turbidity of the culture increases, which results in lower transmitted light. This method can be used to measure the density of the cells, but it cannot measure the viability of the cells as it is not possible to differentiate dead cells from live cells.

With electrochemical impedance spectroscopy (EIS) or dielectric spectroscopy, it is also possible to measure the number of cells in a liquid culture. An additional benefit of this method is that it only measures intact cells. Debris in the cultures is not measured. EIS, therefore, also indicates the viability of the cells in the culture. In EIS the capacitance of two parallel electrodes, placed in the electrolyte medium, is measured under AC perturbation. The microbial cells are surrounded by a membrane which separates the ions inside the cytoplasm from the ions present in the electrolyte medium. When an AC electric field is applied between the two electrodes, the cell becomes polarized, and the ions are separated at the cell membrane. The polarized cell acts as a small capacitor and contributes to the measured capacitance. Every cell has its characteristic frequency at which the cell membrane polarizes. At lower frequency (0.1 MHz), the conductivity of the electrolyte medium contributes to the capacitance value as well. At higher frequency (10 MHz), the cell membrane does not become polarized because of the finite size there is not enough time for charges to build up. Hence, the characteristic frequency to polarize the cell membrane lies between 0.1-10 MHz.

The dielectric spectra of biological tissues and cell suspensions show three kinds of dispersions when exposed to an AC frequency range between 1 Hz and 10 MHz [105-106]. The α dispersion is mostly interfered by the presence of the electrode polarization effects. The β dispersion is due to the interfacial polarization of the cell plasma membrane. The γ dispersion occurs due to a reorientation of water molecules. Hence, the beta dispersion range gives the characteristic dispersive frequency of a cell suspension to calculate the capacitance.

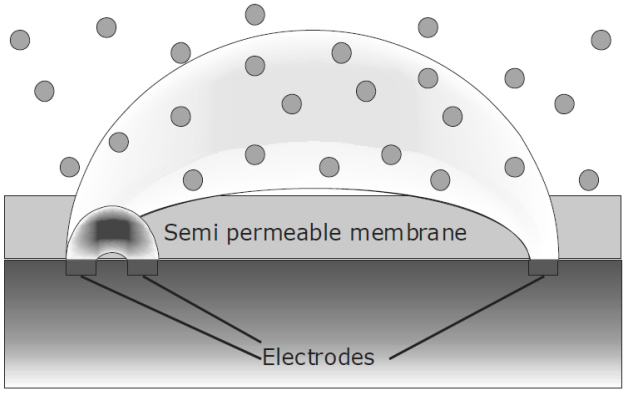

Fig. 2.11: Schematic representation of three-electrode system to measure the cell capacitance

One of the main challenges with impedance-based biomass measurement is the influence of the electrolyte (growth medium) conductivity. The conductivity of the growth medium changes during the growth of the micro-organisms due to the increased concentration of ionic metabolic products, e.g., acetate, lactate. The conductivity change can be compensated by differential impedance measurements using a three-electrode system (Fig. 12). In this method, a pair of electrodes are covered with an ion-permeable membrane, and the other electrode pair is left uncovered. The membrane prevents that the capacitance of the cells is measured between the electrodes and only measures the contribution to the capacitance of the electrolyte. The capacitance of the uncovered electrode pair measures the total capacitance (cells and electrolyte).

The actual cell concentration can be obtained by measuring the capacitance at a frequency below 0.1 MHz and at the frequency characteristic for the specific cells (0.1-10 MHz). The difference between these two values is related to the presence of polarized cell membranes. The more polarized cell membranes, the higher the difference between the two capacitance measurements. Krommenhoek et al (2007), used this method to measure the biomass concentration in a *Saccharomyces cerevisiae* fermentation (6, 10). Fig. 13 shows the conductivity change with respect to the applied frequency (Fig. 13a) and with respect to

biomass concentration (Fig. 13b) of *S. cerevisiae* fermentation medium. The conductivity value is normalized against the conductivity measured at 10 kHz.

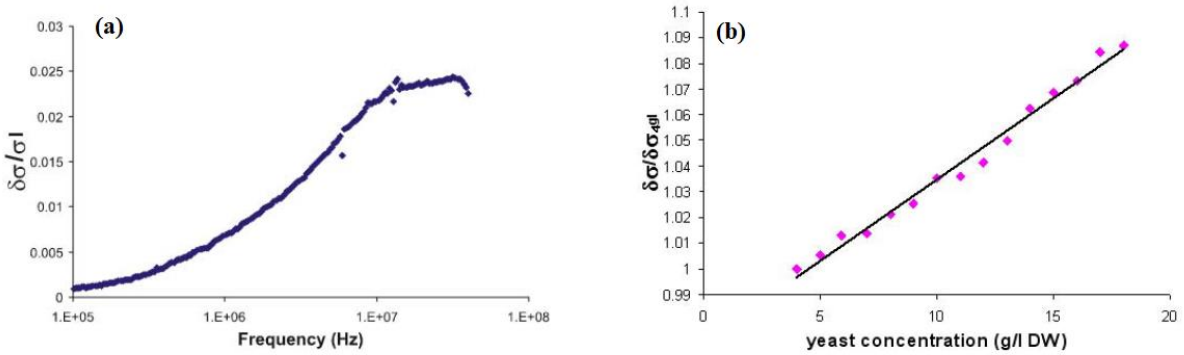

Fig. 2.12: Conductivity change with respect to frequency (a), and biomass concentration (b).

2.4. Sensors for microtiter plate mini-bioreactors

Though there are many sensing techniques available to measure the pH and dissolved oxygen, only a few are compatible with microtiter plate mini-bioreactors. Electrochemical sensors have been used to monitor pH and dissolved oxygen in large scale bioreactors. Their invasiveness, fragility, and large size make that these electrodes are not useful for measurements in microreactor applications.

ISFET pH sensors are useful for microreactors because of their small size and robustness. However, a relatively large reference electrode must be used with an ISFET pH electrode to refer the ISFET potential to. However, this disadvantage has been overcome through the use of microfabrication technology. The ISFET pH sensor chip was embedded in a printed circuit sensor design that was used in an integrated sensor array for eight micro bioreactors. The eight microreactor array was placed on top of a printed circuit board that housed ISFET pH sensors along with other sensors. The device was used to cultivate *Escherichia coli* and monitor the pH during the growth in Luria-Bertani medium [109].

Krommenhoek et al. (2007) developed an integrated sensor array for on-line monitoring of fermentation processes in 96-well MTP microreactors [10]. An ISFET pH electrode, a platinum

microelectrode array for dissolved oxygen, a conductivity electrode for biomass measurements, and a platinum thermistor for temperature measurements were micro-fabricated on a printed circuit board using a photolithographic method. The 96-well MTP is placed on top of the integrated sensor array in such a way that the four different sensors are fixed at the bottom of every single micro-bioreactor. This setup was used to follow online the pH, DO, biomass, and temperature during a Saccharomyces cerevisiae yeast batch-fermentation.

Kosov et al. **(**2001**)** used ratiometric measurements with a pH-sensitive dye based on 1 hydroxypyrene-3,5,7-sulfonic acid (HPTS), pKa 7.2. The dye was excited at 400 and 450 nm, and pH-dependent fluorescence emission at 520 nm was recorded. This radiometric approach was reported to be accurate and free of turbidity interferences during the process. HPTS was added directly to the culture medium. The pH was calibrated by measuring the intensity ratio of the emission of HPTS at 520 nm excited at 400 and 450 nm in solutions with a different pH. In another study, online pH measurements in micro bioreactors were based on radiometric detection of two fluorescent dyes. The pH-sensitive fluorescent and the reference pH insensitive fluorescent dyes with different decay rates were excited at a single wavelength. The ratio of the emission intensities of the fluorophores was measured and a linear relationship between the ratio and pH as obtained in a range between pH 6 and pH 8. To measure DO in a microbioreactor, a sensor film of Ru (diphenylphenanthroline)$_3$.Cl_2 immobilized in silicone rubber was fixed at the wall of the MTP [110].

An improved dual optical sensing method for pH and DO measurements in MTP was reported [111]. In this case, both pH and DO sensitive fluorophores were immobilized in a silicone polymer. The sensor film was created on a polymer support. The prepared sensor patch was fixed at the bottom of the MTP. Kermis et al. (2006) have immobilized pH sensitive HPTS resin beads inside a polyethylene glycol (PEG) hydrogel layer. The HPTS based pH sensor is prepared by drop-casting a hydrogel layer on a white microfiltration membrane [112]. The

HPTS pH sensor and a Ru (diphenylphenanthroline)$_3$.Cl_2 based DO sensor were integrated in a 24-station high throughput microbioreactor sytem. In addition to the sensors, each micro reactor was also equipped with an independent agitator.

John et al. (2003) integrated an optical sensor in an MTP to measure the oxygen transfer rates [113]. A thin sensor film was drop-casted at the bottom of an MTP. The oxygen luminophore ruthenium-(diphenylphenanthrolin)$_3$.Cl_2 was used as the sensing material and safranin was used as a reference dye. The dissolved oxygen concentration was detected using radiometric intensity measurement. The sensing material and reference dye were electrostatically attached to silica gel as shown in Fig. 14. *Corynebacterium glutamicum* were cultivated in 96 MTPs placed in a Fluoroskan Ascent fluorescence reader. They measured a maximal oxygen transfer rate of 7.5 mM h^{-1}.

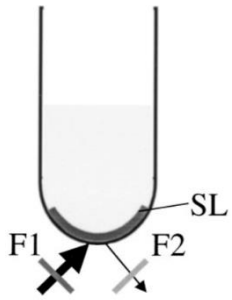

Figure 2.13: An optical sensor spot fixed at the bottom of a round shaped MTP microreactor; SL-sensing layer; F1 filter for excitation light; F2 filter for fluorescence light.

Tang et al. (2006) reported a 24-microtiter plate mini bioreactor system in which control of pH, DO, and temperature was possible for every reactor independently [114]. They used two separate optical sensor films that were fixed at the bottom of the MTP for the measurement of pH and DO. The MTP was a modified 10 ml deep well format to create 10 ml mini-bioreactors, as shown in Fig 15. The MTP was closed with an oxygen permeable membrane to decrease the evaporation rate. This mini-bioreactor system was used to grow *Shewanella oneidensis* MR-1,

and its ability to convert chromium (VI) to less soluble chromium (III) was studied under various environmental conditions.

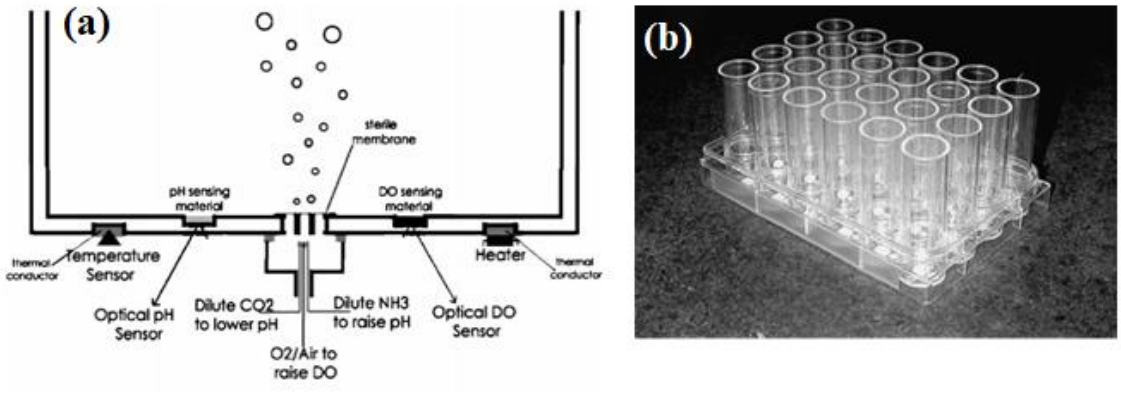

Figure 2.14: Schematic representation of a pH and DO sensor setup in a micro reactor (a), and image of 24-well MTP used for fermentation [114].

Isett et al. (2007) used optically isolated pH and DO sensor patches [115]. They used luminescent quenching of fluorophores by protons and oxygen to measure pH and DO. The fluorophore spots were immobilized in each well of a flat-bottom MTP (Fig.16). The dual reference sensing technology was used. Two fluorescent dyes, one indicator dye and sensitive to pH/DO and one reference dye that is insensitive to pH/DO. The fluorescent dyes were excited at 470 nm for pH and 510 nm for DO. The intensity ratio of the emission spectra was used for the measurement of pH/DO.

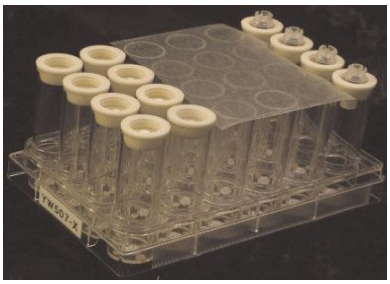

Figure 2.15: A 24-well micro titer plate with a gas permeable cap and silicone polymer membrane [115].

A similar optical sensing arrangement in MTPs was used to study the feasibility of using a 24-well MTP as a scale down tool for cell culture development. Several issues related to cell growth in MTP were observed: A poor oxygen transfer rate, foam formation due to sparging of gases for DO control, and a high evaporation rate. However, the issues were partly overcome by using a lower sparging rate, addition of antifoam agents, and liquid addition for pH control [116-117].

Wolfbeis et al [118] reported further improvements in the optical sensing of pH and DO measurements in MTP. They developed a dual optical sensor to measure pH and DO during bacterial growth in a 24-well MTP (Fig. 17). Unlike previous systems, where separate sensor patches were used for pH and DO measurements, they used a single sensor spot containing both pH and DO sensitive fluorophores encapsulated in organosilica microbeads. The pH fluorophores contains 8-hydroxy- pyrene-1,3, 6-trisulfonate (HPTS) incorporated in methacrylate based polymer matrix and DO fluorophores contains oxygen sensitive ruthenium-tris-4,7-diphenyl-1,10-phenanthroline-di-(trimethylsilylpropanesulfonate) dispersed in organosilica microparticles. A 10-µm sensor film was obtained by knife coating on polyethylene terephthalate, which is used as the sensor spot. The pH and DO measurements were carried out during the growth of *Pseudomonas putida*. The growth kinetics of *P. putida* were successfully studied using these modified 24-well MTPs.

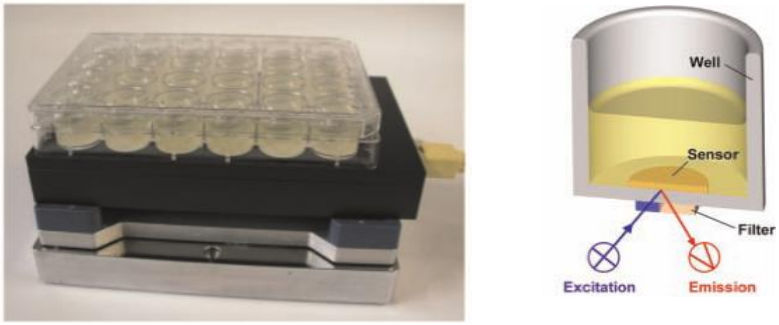

Figure 2.16: Images of 24-microtiter plate; (a) MTP during the bacterial growth, (b) the arrangement of the sensor film contains pH and DO sensor probe. [118]

Dual optical sensing technology reduced the size of the sensor space used for analytical measurements. It resulted in the development of compact micro bioreactors and reduced the production cost of micro bioreactors. Though, the improved development of pH and DO sensors assisted the study of MTP-based micro bioreactors for several applications, still several issues related to sensor stability, accuracy as well as photo bleaching, heat sterilization need to be addressed for potential practical applications.

2.5. References

1. W.Y. Chung, Y.T. Lin, D. G. Pijanowska, C.H. Yang, M. C. Wang, A. Krzyskow, W. Torbicz, New ISFET interface circuit design with temperature compensation. Microelectronics Journal. 37 (2006) 1105-1114.
2. W.Y. Chung, C.H. Yang, D. G. Pijanowska, P.B. Grabiec, W. Torbicz, ISFET performance enhancement by using the improved circuit techniques. Sensors and Actuators B- Chemical 113 (2006) 555-562.
3. S. Jamasb, An analytical technique for counteracting drift in ion-selective field effect transistors (ISFETs). Ieee Sensors Journal 4 (2004) 795-801.
4. S. Jamasb. S. D. Collins, R. L. Smith, A physical model for drift in pH ISFETs. Sensors and Actuators B-Chemical 49 (1998) 146-155.
5. S. Jamasb, S.D. Collins, R. L. Smith, A physical model for threshold voltage instability in Si3N4-gate H+-sensitive FET's (pH ISFET's). IEEE Transactions on Electron Devices 46 (1998) 1239-1245.
6. E. Krommenhoek, Integrated sensor array online monitoring fermentation process, phd thesis, 2007, Enschede, The Netherlands.

7. Southampton electrochemistry group, 2011, Instrumental methods in electrochemistry: woodhead publishing limited.

8. A. J. Bard, L. R. Faulkner, Electrochemical Methods, Fundamentals and Applications: John Wiley & Sons, Inc., (2001)

9. Brett CMA, Brett AMO. 1983. Electrochemistry: Principles, Methods and Applications. New York: Oxford University Press. (1983) 81-90.

10. E. E. Krommenhoek, J. G. E. Gardeniers, J. G. Bomer, X. Li, M. Ottens, G. W. K. van Dedem, M. Van Leeuwen, W. M. van Gulik, L. A. M. van der Wielen, J. J. Heijnen, and A. van den Berg, Integrated Electrochemical Sensor Array for On-Line Monitoring of Yeast Fermentations, Anal. Chem., 79 (2007) 5567–5573

11. W. E. Morf, N. F. de Rooij, Performance of amperometric sensors based on multiple microelectrode arrays. Sensors and Actuators B-Chemical 44 (1997) 538-541.

12. Y. Q. Chen, G. A. Li, A Mathematical-Model with Finite-Element Analysis of Recessed Dissolved-Oxygen Cathode Array. Sensors and Actuators B-Chemical 10 (1993) 223-228.

13. P. Bergveld, Development of an ion-sensitive solid-state device for neurophysiological measurements. IEEE Transactions on Biomedical Engineering 17 (1970) 70-71.

14. P. Bergveld P, Thirty years of ISFETOLOGY - What happened in the past 30 years and what may happen in the next 30 years. Sensors and Actuators B-Chemical 88 (2003) 1- 20.

15. B. A. McKinley**,** ISFET and Fiber Optic Sensor Technologies: In Vivo Experience for Critical Care Monitoring, Chem. Rev. 108 (2008) 826−844

16. B. A. McKinley, J. Saffle, W. S. Jordan, J. Janata, S. D. Moss, D. R. Westenskow, Med. Instrum 14 (1980) 93.

17. B. A. McKinley, B. A. Houtchens, J. Janata, Continuous monitoring of interstitial fluid potassium during hemorrhagic shock in dogs, J. Crit. Care Med. 9 (1981) 845.

18. A. Haemmerli, J. Janata, H. M. Brown, on-selective electrode for intracellular potassium measurements, Anal. Chem. 52 (1980) 1179.

19. P. T. McBride, J. Janata, P. A. Comte, S.D. Moss, C. C. Johnson, Ion-selective field effect transistors with polymeric membranes, Anal. Chim. Acta 101 (1978) 239.

20. S. D. Moss, C. C. Johnson, J. Janata, Hydrogen, calcium, and potassium ion-sensitive FET transducers: a preliminary report. IEEE Trans. Biomed. Eng. 1978, 25, 49.

21. B. A. McKinley, K. C. Wong, J. Janata, W. S. Jordan, D. R. Westenskow, In vivo continuous monitoring of ionized calcium in dogs using ion sensitive field effect transistors. Crit. Care Med. 9 (1981) 333.

22. B. A. McKinley, C. L. Parmley, W. P. Morris, S. J. Allen, A. S. Tonnesen, Technology report: Continuous in vivo arterial blood gas monitor systems, University Hospital Consortium Clinical Practice Advancement Center, 1994.

23. D. Wencel, T. Abel, and C. McDonagh, Optical Chemical pH Sensors, Anal. Chem. 86 (2014) 15−29.

24. M. J. P. Leiner and P. Hartmann, Theory and practice in optical pH sensing, Sensors and Actuators B, 11 (1993) 281-289.

25. J. Lin, D. Liu, An optical pH sensor with a linear response over a broad range, Analytica Chimica Acta 408 (2000) 49–55.

26. Jiri Janata, Do Optical Sensors Really Measure pH?, ANALYTICAL CHEMISTRY, VOL. 59, 9, MAY 1, 1987

27. J. Han and K. Burgess, Fluorescent Indicators for Intracellular pH, Chem. Rev. 110 (2010) 2709–2728

28. V. Vojinovic, J.M.S. Cabral, L.P. Fonseca, Real-time bioprocess monitoring Part I: In situ sensors, Sensors and Actuators B 114 (2006) 1083–1091

29. J. R. Lakowicz, Principles of Fluorescence Spectroscopy, 3rd ed. Springer-Verlag: New York, 2006.

30. I. Klimant, Method and Device for Referencing Fluorescence Intensity Signals. U.S. Patent 6 (2003) 602.

31. Borisov, S. M.; Gatterer, K.; Klimant, I. Red light-excitable dual lifetime referenced optical pH sensors with intrinsic temperature compensation, Analyst 135 (2010) 1711−1717.

32. Borisov SM, Neurauter G, Klimant I, Wolfbeis OS. A modified dual lifetime referencing method for simultaneous optical determination and sensing of two analytes. Appl Spectrosc 60 (2006) 1167–1173.

33. A. S. Vasylevska, S. M. Borisov, C. Krause, O. S. Wolfbeis, Indicator-loaded and permeation-selective microparticles for use in fiber optic simulta- neous sensing of ph and dissolved oxygen. Chem Mater 18 (2006) 4609–4616.

34. A. S. Kocincova, S. Nagl, S. Arain, C. Krause, S. M. Borisov, M. Arnold, O. S. Wolfbeis, Multiplex Bacterial Growth Monitoring in 24-Well Microplates Using a Dual Optical Sensor for Dissolved Oxygen and pH Biotechnology and Bioengineering, 100 (2008) 430.

35. E. Bakker, P. Buhlmann, E. Pretsch, Carrier-Based Ion-Selective Electrodes and Bulk Optodes. 1. General Characteristics, **Chem. Rev.** 97 (1997) 3083.

36. P. Bühlmann, E. Pretsch, E. Bakker, Carrier-based ion-selective electrodes and bulk optodes. Ionophores for potentiometric and optical sensors. Chem Rev. 98 (1998) 1593-1687.

37. P. Buhlmann, Y. Umezawa, S. Rondinini, Lifetime of ion-selective electrodes based On charged ionophores. Anal Chem. 72 (2000) 1843- 1852.

38. S. Amemiya, P. Bühlmann, E. Pretsch, Cationic or anionic sites? Selectivity optimization of ion-selective electrodes based on charged ionophores. Anal Chem. 72 (2000) 1618-1631.

39. K. Mikhelson, A. Lewenstam, Modeling of divalent/monovalent ion selectivity of ionexchanger-based solvent polymeric membranes doped with coexchanger, Anal Chem. 72 **(**2000) 4965-4972.

40. T. Rosatzin, E. Bakker, K. Suzuki, Lipophilic and immobilized anionic additives in solvent polymeric membranes of cation-selective chemical sensors. Anal Chim Acta. 280 **(**1993) 197-208.

41. C. Moore, B. C. Pressmann, Biochem. Biophys. Mechanism of action of valinomycin on mitochondria, Res. Commun. 15 (1964) 562.

42. (a) C. J. Pedersen, Cyclic polyethers and their complexes with metal salts, J. Am. Chem. Soc. 89 (1967) 2495-2496. (b) C. J. Pedersen, Cyclic polyethers and their complexes with metal salts, J. Am. Chem. Soc. 89 (1967) 7017-7036; (c) C. J. Pedersen, Cyclic polyethers and their complexes with metal salts, J. Am. Chem. Soc. 92 (1970) 386-391; (d) C. J. Pedersen, Cyclic polyethers and their complexes with metal salts, J. Am. Chem. Soc. 92 (1970) 391-394.

43. B. Dietrich, J. M. Lehn, J. P. Sauvage, Diaza-Poloxo-Macrocycles et macrobicycles, J. P. Tetrahedron Lett. 34 (1969) 2885.

44. J. M. Lehn, J. P. Sauvage, J. Chem. Soc., Cation and cavity selectivities of alkali and alkaline-earth "cryptates", Chem. Commun. 9 (1971) 440.

45. Dobler, M. Ionophores and their Structures; Wiley-Interscience: New York, 1981.

46. D. Ammann, E. Pretsch, W. Simon, A synthetic, electrically neutral carrier for Ca, Tetrahedron Lett. 124 (1972), 2473.

47. D. Ammann, E. Pretsch, W. Simon, A Calcium Ion-Selective Electrode Based on a Neutral Carrier, Anal. Lett. 5 (1972) 843.

48. D. Ammann, P. Anker, P. C. Meier, W. E. Morf, E. Pretsch, W. Simon, Neutral Carrier Based Ion-Selective Electrodes, Ion-Sel. Electr. Rev. 5 (1983) 3.

49. O. H. LeBlanc, J. F. Brown, J. F. Klebe, L. W. Niederach, G. M. J. Slusarczuk, W. H. Stoddard, Polymer membrane sensors for continuous intravascular monitoring of blood pH, J. Appl. Physiol. 40 (1976) 644.

50. R. L. Coon, N. C. Lai, J. P. Kampine, Evaluation of a dual-function pH and P_{CO2} in vivo sensor, J. Appl. Physiol. 40 (1976) 625.

51. M. C. Harman, P. A. Poole-Wilson, A liquid ion-exchange intracellular pH micro-electrode, J. Appl. Physiol. 315 (1981) 16.

52. P. Schulthess, Y. Shijo, H. V. Pham, E. Pretsch, D. Ammann, W. Simon, A hydrogen ion-selective liquid-membrane electrode based on tri-*n*-dodecylamine as neutral carrier, Anal. Chim. Acta 131 (1981) 111.

53. D. Ammann, F. Lanter, R. A. Steiner, P. Schulthess, Y. Shijo, W. Simon, Neutral carrier based hydrogen ion selective microelectrode for extra- and intracellular studies, Anal. Chem. 53 (1981) 2267.

54. O. Dinten, U. E. Spichiger, N. Chaniotakis, P. Gehrig, B. Rusterholz, W. E. Morf, W. Simon, Lifetime of neutral-carrier-based liquid membranes in aqueous samples and blood and the lipophilicity of membrane components, Anal. Chem. 63 (1991) 596.

55. E. Lindner, V. V. Cosofret, R. P. Buck, T. A. Johnson, R. B. Ash, M. R. Neuman, W. J. Kao, J. M. Anderson, Electroanalytical and biocompatibility studies on microfabricated array sensors, Electroanalysis 7 (1995) 864.

56. D. Liu, M. E. Meyerhoff, H. D. Goldberg, R. B. Brown, Potentiometric ion- and bioselective electrodes based on asymmetric polyurethane membranes, Anal. Chim. Acta 274 (1993) 37.

57. P. Chao, D. Ammann, U. Oesch, W. Simon, F. Lang, Extra- and intracellular hydrogen ion-selective microelectrode based on neutral camers with extended pH response range in acid media, Plu¨ gers Arch. 1988, 411, 216.

58. U. Oesch, D. Ammann, Z. Brzo´zka, H. V. Pham, E. Pretsch, B. Rusterholz, W. Simon, G. Suter, D. H. Welti, A. P. Xu, Design of neutral hydrogen ion carriers for solvent polymeric membrane electrodes of selected pH range, Anal. Chem. 1986, 58, 2285.

59. J. Chojnacki, J. F. Biernat, Application of azoles as neutral carriers in liquid membrane ion-selective pH electrodes, J. Electroanal. Chem. 277 (1990) 159.

60. V. M. Lutov, K. N. Mikhelson, A new pH sensor with a PVC membrane: Analytical evaluation and mechanistic aspects, Sens. Actuators, B 1994, 19, 400-403

61. N. Haack, S. Durry, K. W. Kafitz, M. Chesler, C. R. Rose, Double-barreled and Concentric Microelectrodes for Measurement of Extracellular Ion Signals in Brain Tissue, J. Vis. Exp. 103 (2015) 53058.

62. N. Fedirko, N. Svichar, and M. Chesler, Fabrication and Use of High-Speed, Concentric H- and Ca-Selective Microelectrodes Suitable for In Vitro Extracellular Recording, *J Neurophysiol* 96 (2006) 2006.

63. N. Fedirko, N. Svichar, and M. Chesler, Fabrication and Use of High-Speed, Concentric H- and Ca-Selective Microelectrodes Suitable for In Vitro Extracellular Recording, *J Neurophysiol* 96 (2006) 919–924.

64. M. D. Johnson, O. E. Kao, D. R. Kipke, Spatiotemporal pH dynamics following insertion of neural microelectrode arrays, Journal of Neuroscience Methods 160 (2007) 276–287.

65. S. Nakata, T. Arie, S. Akita, and K. Takei, Wearable, Flexible, and Multifunctional Healthcare Device with an ISFET Chemical Sensor for Simultaneous Sweat pH and Skin Temperature Monitoring, ACS Sens. 2 (2017) 443−448.

66. K. Matsuura, Y. Asano, A. Yamada and K. Naruse, Detection of Micrococcus Luteus Biofilm Formation in Microfluidic Environments by pH Measurement Using an Ion-Sensitive Field-Effect Transistor, Sensors 13 (2013) 2484-2493.

67. M. L. Pourciel-Gouzy, W. Sant, I. Humenyuk, L. Malaquin, X. Dollat, and P. Temple-Boyer, Development of pH-ISFET sensors for the detection of bacterial activity. Sens. Actuators, B 103 (2004) 247−251.

68. M. Castellarnau, N. Zine, J. Bausells, C. Madrid, A. Juaŕez, J. Samitier, and A. Errachid, ISFET-based biosensor to monitor sugar metabolism in bacteria. Mater. Sci. Eng., C 28, (2008) 680−685.

69. M. A. Makos, D. M. Omiatek, A. G. Ewing, and M. L. Heien, Development and Characterization of a Voltammetric Carbon-Fiber Microelectrode pH Sensor, Langmuir 26 (2010), 10386–10391

70. P. Takmakov, M. K. Zachek, R. B. Keithley, E. S. Bucher, G. S. McCarty, and R. M. Wightman, Characterization of Local pH Changes in Brain Using Fast Scan Cyclic Voltammetry with Carbon Microelectrodes, Anal. Chem. 82 (2010) 9892–9900.

71. B. J. Venton, D. J.Michael and R. M. Wightman, Correlation of local changes in extracellular oxygen and pH that accompany dopaminergic terminal activity in the rat caudate–putamen, Journal of Neurochemistry, 84 (2003) 373–381.

72. A. K. Dengler, R. M. Wightman, and G. S. McCarty, Microfabricated Collector-Generator Electrode Sensor for Measuring Absolute pH and Oxygen Concentrations, Anal. Chem. 87 (2015) 10556−10564.

73. X. Liu, M. Zhang, T. Xiao, J. Hao, R. Li, and L. Mao, Protein Pretreatment of Microelectrodes Enables in Vivo Electrochemical Measurements with Easy Precalibration and Interference-Free from Proteins, Anal. Chem. 88 (2016) 7238−7244.

74. J. Hao, T. Xiao, F. Wu, P. Yu, and L. Mao, High Antifouling Property of Ion-Selective Membrane: toward In Vivo Monitoring of pH Change in Live Brain of Rats with MembraneCoated Carbon Fiber Electrodes, Anal. Chem. 88 (2016) 11238−1124.

75. R. A. Linsenmeier, and C. M. Yancey, Improved fabrication of double-barreled recessed cathode O2 microelectrodes, 63 (1987) 2554-2557.

76. J.H. Lee, T.S. Lima, Y. Seo, P. L. Bishop, I. Papautsky, Needle-type dissolved oxygen microelectrode array sensors for in situ measurements Sensors and Actuators B 128 (2007) 179–185.

77. J. H. Lee, Y. W. Seo, T.S. Lim, P. L. Bishop, and I. Papautsky, MEMS Needle-type Sensor Array for in Situ Measurements of Dissolved Oxygen and redox Potential, Environ. Sci. Technol., 41 (2007) 7857–7863

78. F. Rossem, J. G. Bomer, H. L. de Boer, Y. Abbas, Eddy de Weerd, A. Berga, Séverine Le Ga, Sensing oxygen at the millisecond time-scale using an ultra-microelectrode array (UMEA), Sensors and Actuators B 238 (2017) 1008–1016.

79. Y. P. Chena, Y. Zhao, J. Chua, S. Y. Liu, W. W. Li, G. Liu, Y. C. Tianc, Y. Xiong, Han-Qing Yu, Fabrication and characterization of an innovative integrated solid-state microelectrode Electrochimica Acta 55 (2010) 5984–5989.

80. Shao-Yang Liu, Gang Liu, Yang-Chao Tian, You-Peng Chen, Han-Qing Yu, and, An Innovative Microelectrode Fabricated Using Photolithography for Measuring Dissolved Oxygen Distributions in Aerobic Granules, Environ. Sci. Technol., 2007, 41 (15), 5447–5452.

81. Hitoshi Shiku, Takuo Shiraishi, Hiroaki Ohya, Tomokazu Matsue, Hiroyuki Abe, Hiroyoshi Hoshi, and Masato Kobayash, Oxygen Consumption of Single Bovine Embryos Probed by Scanning Electrochemical Microscopy, Anal. Chem. 2001, 73, 3751-3758.

82. J. R. Trimarchi, L. Liu, D. M. Porterfield, Peter J.S. Smith, and D. L. Keefe, Oxidative Phosphorylation-Dependent and -Independent Oxygen Consumption by Individual

Preimplantation Mouse Embryos, BIOLOGY OF REPRODUCTION 62 (2000) 1866–1874.

83. D. Wencel, T. Abel, and C. McDonagh, Optical Chemical pH Sensors, Anal. Chem. 86 (2014) 15−29.

84. B. J. Venton, D. J. Michael, R. M. Wightman, Correlation of local changes in extracellular oxygen and pH that accompany dopaminergic terminal activity in the rat caudate–putamen, J. Neurochem. 84 (2003) 373–381.

85. F. B. Bolger, J. P. Lowry, Brain Tissue Oxygen: In Vivo Monitoring with Carbon Paste Electrodes, Sensors 5 (2005) 473–487.

86. A. Song, S. Parus, and R. Kopelman, High-Performance Fiber-Optic pH Microsensors for Practical Physiological Measurements Using a Dual-Emission Sensitive Dye, Anal. Chem. 69 (1997) 863-867.

87. S. M. Grist, L. Chrostowski and K. C. Cheung, Optical Oxygen Sensors for Applications in Microfluidic Cell Culture, Sensors 10 (2010) 9286-9316.

88. E. Betzig, J. K. Troutman, T. D. Harris, J. S. Weiner, R. L. Kostelak, Breaking the Diffraction Barrier: Optical Microscopy on a Nanometric Scale, Science 251 (1991) 1468.

89. W. Tan, R. Kopelman, L. R. Susan, B. Michael, T. Miller, Ultra small optical sensors for cellular, optical measurements, Analytical Chemistry News & Features, September 1, 199, 606 A.

90. S. McCulloch D. Uttamchandani, Development of a fibre optic micro-optrode for intracellular pH measurements, IEE Proc. Optoelectronics 144 (1997) 162-216.

91. A. Song, S. Parus, and R. Kopelman, High-Performance Fiber-Optic pH Microsensors for Practical Physiological Measurements Using a Dual-Emission Sensitive Dye, Anal. Chem. 69 (1997) 863-867.

92. Y. Amao , Probes and Polymers for Optical Sensing of Oxygen, Microchim. Acta 143 (2003) 1–12.

93. Y. Amao, T. Miyashita, I. Okura, Optical oxygen detection based on luminescence change of metalloporphyrins immobilized in poly(isobutylmethacrylate-co-trifluoroethylmethacrylate) film, Analytica Chimica Acta 421 (2000) 167–174.

94. Y. Xiong, J. Xu, D. Q. Zhu, C. F. Duan, Y. F. Guan, Fiber-optic fluorescence sensor for dissolved oxygen detection based on fluorinated xerogel immobilized with ruthenium (II) complex, J. Sol−Gel Sci. Technol. 53 (2010) 441.

95. E. J. Park, K. R. Reid, W. Tang, R. T. Kennedy and R. Kopelman, Ratiometric fiber optic sensors for the detection of inter- and intra-cellular dissolved oxygen J. Mater. Chem., 15 (2005) 2913–2919.

96. W. Tan, Z. Y. Shi, and R. Kopelman, Development of Submicron Chemical Fiber Optic Sensors Anal. Chem. 64 (1992) 2985-2990.

97. A. S. Kocincova, S. M. Borisov, C. Krause, and O. S. Wolfbeis, Fiber-Optic Microsensors for Simultaneous Sensing of Oxygen and pH, and of Oxygen and Temperature, Anal. Chem. 79 (2007) 8486-8493.

98. W. Tan, Z. Y. Shi, S. Smith, D. Birnbaum, R. Kopelman, Submicrometer Intracellular Chemical Optical Fiber Sensors, Science 258 (1992) 778-781.

99. J. F. McCarthy, Development and evaluation of a fluorescence emission ration based fiber optic pH measurement system for use in monitoring changes in tumor pH during clinical hyperthermia, Ph.D. Thesis, University of Illinois, Urbana, IL, 1989.

100. L. Saari, W. R. Seitz, pH sensor based on immobilized fluoresceinamine, Anal. Chem. 54 (1982) 821-823.

101. J. W. Parker, O. Laksin, C. Yu, M. L. Lau, S. Klima, R. Fisher, I. Scott, B. Atwater, Fiber-optic sensors for pH and carbon dioxide using a self-referencing dye, Anal. Chem. 65 (1993) 2329-2334.

102. K.. P. McNamara, X. Li, A. D. Stull, Z. Rosenzweig, Fiber-optic oxygen sensor based on the fluorescence quenching of tris (5-acrylamido, 1,10 phenanthroline) ruthenium chloride Analytica Chimica Acta 361 (1998) 73-83.

103. A. Heller, L. H. Fischer, O. S. Wolfbeis, A. Goepferich, Long time monitoring of the respiratory activity of isolated mitochondria, EXPERIMENTAL CELL RESEARCH 318 (2012) 1667–1672.

104. A. S. Kocincova, S. Nagl, S. Arain, C. Krause, S. M. Borisov, M. Arnold, O. S. Wolfbeis, Multiplex Bacterial Growth Monitoring in 24-Well Microplates Using a Dual Optical Sensor for Dissolved Oxygen and pH, Biotechnology and Bioengineering, 100 (2008) 430.

105. K. Asami, Characterization of biological cells by dielectric spectroscopy. Journal of Non- Crystalline Solids 305 (2002) 268- 277.

106. K. Asami, T. Yonezawa, Dielectric Analysis of Yeast- Cell Growth. Biochimica Et Biophysica Acta- General Subjects 1245 (1995) 99-105.

107. S. A. Siano, Biomass measurement by inductive permittivity. Biotechnology and Bioengineering 55 (1997) 289-304.

108. A. R. Varlan, P. Jacobs, W. Sansen, New design technique for planar conductometric haematocrit sensors. Sensors and Actuators B Chemical 34 (1996) 258-264.

109. M. M. Maharbiz, W. J. Holtz, R. T. Howe, J. D. Keasling, Microbioreactor Arrays With Parametric Control for High-Throughput Experimentation Biotechnol Bioeng 85 (2004) 376-381.

110. Y. Kostov, P. Harms, L. R. Eichhorn, G. Rao, Low-Cost Microbioreactor for High-Throughput Bioprocessing Biotechnol Bioeng 72 (2001) 346-352.

111. H. R. Kermis, Y. Kostov, P. Harms, and G. Rao, Dual Excitation Ratiometric Fluorescent pH Sensor for Noninvasive Bioprocess Monitoring: Development and Application, Biotechnol. Prog. 18 (2002) 1047−1053.

112. P. Harms, Y. Kostov, J. A. French, M. Soliman, M. Anjanappa, A. Ram, G. Rao, Design and Performance of a 24-Station High Throughput Microbioreactor, Biotechnol Bioeng 93 (2006) 6-13.

113. G. T. John, I. Klimant, C. Wittmann, E. Heinzle, Integrated Optical Sensing of Dissolved Oxygen in Microtiter Plates: A Novel Tool for Microbial Cultivation, Biotechnology and Bioengineering, 81 (2003) 829.

114. Y. J. Tang, D. Laidlaw, K.Gani, J.D. Keasling, Evaluation of the effects of various Culture Conditions on Cr(VI) Reduction by Shewanella oneidensis MR-1 in a Novel High-Throughput Mini-Bioreactor, Biotechnol Bioeng 95 (2006) 176–184.

115. K. Isett, G. H. Herber, A. Amanullah, Twenty-four-well plate miniature bioreactor high-throughput system: Assessment for microbial cultivations. Biotechnol Bioeng 98 (2007) 1017–1028.

116. A. Chen, R. Chitta, D. Chang, A. Amanullah, Twenty-Four Well Plate Miniature Bioreactor System as a Scale-Down Model for Cell Culture Process Development, Biotechnol Bioeng 102 (2009) 148-160.

117. A. S. Kocincova, S. Nagl, S. Arain, C. Krause, S. M. Borisov, M. Arnold, O. S. Wolfbeis, Multiplex Bacterial Growth Monitoring in 24-Well Microplates Using a Dual Optical Sensor for Dissolved Oxygen and pH, Biotechnology and Bioengineering, 100 (2008) 430.

118. S. Arain, G. T. John, C. Krause, J. Gerlach, O. S. Wolfbeis, I. Klimant, Characterization of microtiterplates with integrated optical sensors for oxygen and pH, and their applications to enzyme activity screening, respirometry, and toxicological assays, Sensors and Actuators B 113 (2006) 639–648.